

Theory of four-wave-mixing in phonon polaritons

Christopher R. Gubbin and Simone De Liberato

*School of Physics and Astronomy, University of Southampton,
Southampton, SO17 1BJ, United Kingdom*

Abstract

Third order anharmonic scattering in light-matter systems can drive a wide variety of practical and physically interesting processes from lasing to polariton condensation. In this Letter we develop a quantum theory capable of describing such processes in arbitrarily inhomogeneous photonic environments. Motivated by recent experimental results in the nonlinear optics of localised phonon polaritons, we investigate four-wave mixing in those systems, whose modes possess ultrasmall mode volumes and narrow linewidths. In particular we study self-phase-modulation and parametric scattering, showing both processes to be within experimental reach.

I. INTRODUCTION

Polaritons are quasiparticle excitations arising from strong coupling between light and matter. They inherit the best properties of both constituents, being light and fast but also strongly interacting and therefore present an ideal platform for nonlinear photonics. In microcavity polariton systems [1, 2], four-wave-mixing processes mediated by the Coulomb interaction between the underlying exciton degrees of freedom allow for realization of polariton condensation [3, 4] and superfluidity [5, 6] as well as of practical devices such as polariton parametric oscillators [7, 8] and electrically pumped polariton lasers [9, 10].

When photons hybridise with coherent charge oscillations close to an interface, the resulting polariton modes can be evanescent and localised on sub-wavelength scales. Plasmon polaritons on the surface of noble metals are archetypes of such localised excitations, but their lossy character, due to strong intrinsic Ohmic heating, have until now limited their practical applications [11]. Phonon polaritons, whose matter component is due to the ions of a polar dielectric, represent in this sense an interesting low loss option, covering the mid-infrared spectral region [12]. Not only have these been exploited for coherent thermal emission [13], but more recently tunable, localized resonances in Silicon Carbide (SiC) resonators have been observed [14–16], with quality factors far exceeding the theoretical limit for plasmon polaritons. Localized phonon polaritons therefore present an ideal platform to translate established plasmonic and polaritonic technology to the mid-infrared. In order to quantify the potential of surface phonon polaritons for mid-infrared nonlinear and quantum optics we recently developed a real space Hopfield-like [17] framework which allows for quantisation and diagonalisation of arbitrary inhomogeneous systems in terms of polaritonic excitations whose field profile can be obtained by solving inhomogeneous Maxwell equations [18]. Such a theory allows us to quantitatively describe scattering between different polaritonic modes in systems with nanoscopic inhomogeneity, which we initially exploited to model early second harmonic generation experiments on flat SiC surfaces [19]. Such nonlinear processes have now been demonstrated experimentally utilising thick SiC substrates in reflectance [20], from sub-diffraction surface phonon polaritons excited by prism coupling [21], and from arrays of discrete SiC nano-resonators [22].

In this Letter, building on our previous results and with the intent to design practical mid-infrared nonlinear polariton devices, we develop the theory of phonon polariton four-

wave-mixing, demonstrating that two important applications are within experimental reach with available sources. The first, self-phase-modulation [23], would be the first experimental verification of third order nonlinearities in SiC, allowing us to experimentally fix the material scattering parameters beyond current best estimates based on *ab initio* simulation [24]. The second, polaritonic scattering in a parametric oscillator configuration, will demonstrate the viability of SiC phonon polariton resonators for mid-infrared quantum polaritonic and nonlinear optics.

II. THEORY OF POLARITONIC SCATTERING

The quadratic Hamiltonian of a generally inhomogeneous light-matter system can be diagonalized introducing the bosonic operators $\hat{\mathcal{K}}_{\mathbf{p}}$ as

$$\hat{\mathcal{H}}_0 = \sum_{\mathbf{p}} \hbar \omega_{\mathbf{p}} \hat{\mathcal{K}}_{\mathbf{p}}^\dagger \hat{\mathcal{K}}_{\mathbf{p}}, \quad (1)$$

where the index \mathbf{p} runs over all the coupled system spectrum including *a priori* both discrete and continuous components [18]. The general third-order nonlinear Hamiltonian mediated by the susceptibility $\chi^{(3)}$ has the form

$$\hat{\mathcal{H}}^{(3)} = \epsilon_0 \sum_{ijkl} \sum_{[\mathbf{p}_1-\mathbf{p}_4]} \int d\mathbf{r} \chi_{ijkl}^{(3)}(\omega_{\mathbf{p}_1}, \omega_{\mathbf{p}_2}, \omega_{\mathbf{p}_3}, \omega_{\mathbf{p}_4}) \Upsilon(\mathbf{r}) \hat{\mathbf{E}}_{\mathbf{p}_1}^i(\mathbf{r}) \hat{\mathbf{E}}_{\mathbf{p}_2}^j(\mathbf{r}) \hat{\mathbf{E}}_{\mathbf{p}_3}^k(\mathbf{r}) \hat{\mathbf{E}}_{\mathbf{p}_4}^l(\mathbf{r}), \quad (2)$$

where we assumed a single material with third-order nonlinear susceptibility tensor $\chi_{ijkl}^{(3)}$ whose spatial variation is described by $\Upsilon(\mathbf{r})$. Vector components are denoted by i, j, k, l , and we denote electric field of the four participating modes $\hat{\mathbf{E}}_{\mathbf{p}}(\mathbf{r})$ which are related simply to the polaritonic operators as

$$\hat{\mathbf{E}}_{\mathbf{p}}(\mathbf{r}) = \sqrt{\frac{\hbar \omega_{\mathbf{p}}}{\epsilon_0 V_{\mathbf{p}}}} \left(\bar{\boldsymbol{\alpha}}_{\mathbf{p}}(\mathbf{r}) \hat{\mathcal{K}}_{\mathbf{p}} + \boldsymbol{\alpha}_{\mathbf{p}}(\mathbf{r}) \hat{\mathcal{K}}_{\mathbf{p}}^\dagger \right), \quad (3)$$

where $\boldsymbol{\alpha}_{\mathbf{p}}(\mathbf{r})$ are the Hopfield coefficients obtained solving the Maxwell equations in the inhomogeneous system and $V_{\mathbf{p}}$ is the classical photonic mode volume.

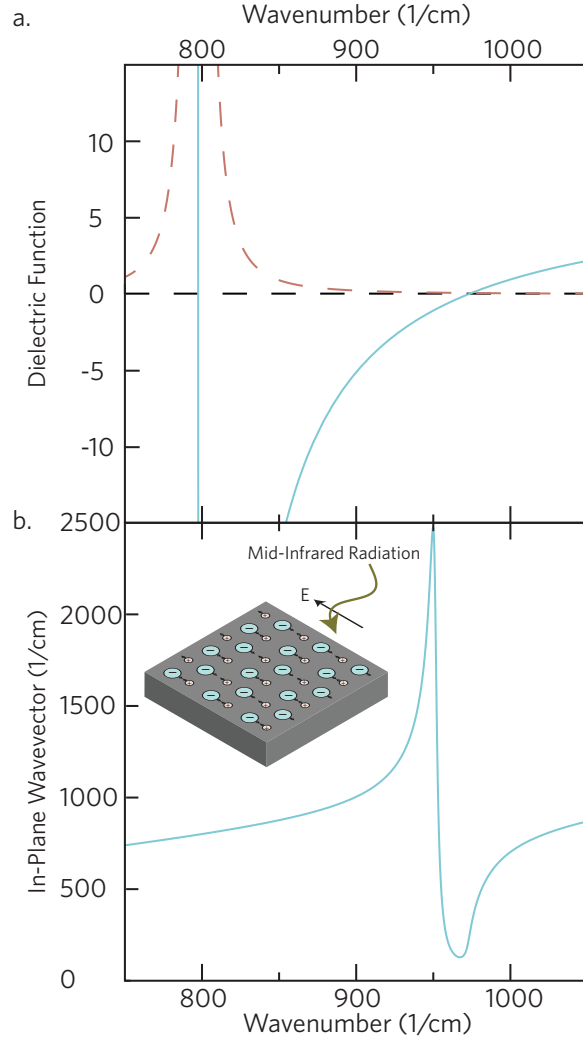


FIG. 1. a. The dielectric function of β -SiC. The real component (blue solid line) is negative between the transverse optic phonon resonance at 797/cm and the longitudinal optic phonon resonance at 972/cm. b. Dispersion of the evanescent mode of a β -SiC halfspace. Inset shows an illustration of the interaction of an impinging electric field with a polar dielectric's ionic lattice .

III. FOUR-WAVE MIXING USING PHONON POLARITONS

In this Letter we study four-wave mixing processes utilising surface phonon polaritons in β -SiC, a polytype of SiC with zincblende morphology. Polar dielectrics like β -SiC support surface phonon polaritons in the region where their dielectric function $\epsilon(\omega) < 0$. The dielectric function of β -SiC is illustrated in Fig. 1a, the real component clearly changing sign at $\omega_{TO} = 797.5/\text{cm}$ and at $\omega_{LO} = 972/\text{cm}$, the transverse and longitudinal optic phonon

frequencies marking the crystals Reststrahlen band.

Surface phonon polaritons allow sub-diffraction light localisation by transient storage of energy in the kinetic and potential energy of the ionic lattice. The surface distortion induced by an impinging electric field is illustrated in the inset of Fig. 1b. In simple systems such as a β -SiC halfspace in vacuum the surface phonon polariton spectrum can be calculated analytically, the dispersion of this propagative mode is shown in Fig. 1b. In more complex geometries such as three-dimensional nanoscopic resonators the spectrum can be calculated numerically [14].

Surface phonon polaritons are especially promising as a platform for mid-infrared nonlinear optics as a result of their ultra-low mode volumes, high quality factors, and the intrinsic anharmonicity of the host polar dielectric. As we lack measurements or *ab initio* calculations of the necessary nonlinear parameters for β -SiC, in this Letter we utilise the results of Vanderbilt *et al.*, who studied second and third order anharmonic scattering in systems with a diamond crystal structure, observing a universality in coefficients governing the mechanical anharmonicity on rescaling by the bond length and spring constant [24]. Our recent results demonstrate that these results are applicable to β -SiC at least for second order nonlinearities, and we expect they should provide reasonable estimates also for third order ones. Intriguingly, the predicted third-order nonlinear anharmonic scattering coefficients are attractive, contrasting the repulsive material interactions in microcavity polariton systems. [19]. As all modes participating in the processes studied in this letter lie in the Reststrahlen band, in the neighbourhood of the fourth order pole in the mechanical $\chi^{(3)}$, we ignore lower order contributions to the optical nonlinearity. Furthermore as only the $xxxx, xyxy, xxyy$ components of the nonlinear tensor are non-zero for tetragonal configurations such as β -SiC [24] we are able to simplify Eq. 2 dramatically.

In nonlinear optical experiments the available pump fluency is of course the key parameter which determining which phenomena are within experimental reach. We will thus use parameters representative of the free-electron laser previously utilized to probe $\chi^{(2)}$ nonlinearities in polar dielectrics by the group of A. Paarmann [21], specifically a pulsed excitation of duration 1pS, energy $2\mu\text{m}$, and an elliptical excitation spot with semi-major and semi-minor axes $500\mu\text{m}$ and $150\mu\text{m}$ respectively.

A. Self-Phase-Modulation

Self-phase-modulation is an intensity dependant frequency shift due to the excitations self-interaction. This can be understood by taking the nonlinear Hamiltonian Eq. 2, specialising onto the case of self-interaction ($\mathbf{p}_j = \mathbf{p} \ \forall j$) and, considering a pump beam, linearising by the standard substitution $\hat{\mathcal{K}}_{\mathbf{p}} \rightarrow \sqrt{\mathcal{M}}$ where \mathcal{M} is the population in the mode under consideration. This results in a quadratic Hamiltonian with new modal frequencies $\omega'_{\mathbf{p}} = \omega_{\mathbf{p}} (1 + \Delta_{\mathbf{p}})$ where the fractional shift is given by

$$\Delta_{\mathbf{p}} = \frac{3\hbar\omega_{\mathbf{p}}\mathcal{M}}{\epsilon_0} \sum_{ijkl} \chi_{ijkl}^{(3)}(\omega_{\mathbf{p}}, \omega_{\mathbf{p}}, \omega_{\mathbf{p}}, \omega_{\mathbf{p}}) \frac{\mathcal{V}_{\mathbf{pp}}}{V_{\mathbf{p}}^2}, \quad (4)$$

and we defined an effective interaction volume in terms of the Hopfield coefficients as

$$\mathcal{V}_{\mathbf{p}_1 \mathbf{p}_2}^{\mathbf{p}_3 \mathbf{p}_4} = \int d\mathbf{r} \ \Upsilon(\mathbf{r}) \alpha_{\mathbf{p}_1}^i(\mathbf{r}) \alpha_{\mathbf{p}_2}^j(\mathbf{r}) \bar{\alpha}_{\mathbf{p}_3}^k(\mathbf{r}) \bar{\alpha}_{\mathbf{p}_4}^l(\mathbf{r}). \quad (5)$$

In order to assess whether such effects are observable we consider two 1D inhomogeneous systems, consisting of either a planar β -SiC halfspace (inset of Fig. 2a) or a β -SiC film grown on a deep SiO_2 substrate [25] (inset of Fig. 2b). The halfspace system supports a single evanescent surface phonon polariton while the film supports dual modes, understood as anti-symmetric and symmetric superpositions of the surface phonons at each interface. The modes of the system, found considering the poles of the reflection coefficients for the stack, are shown in Fig. 2a and b for the bilayer system and a SiC film of thickness 100nm on a thick SiO_2 substrate. Utilising Eq. 4 we may now calculate the expected fractional frequency shifts, shown in Fig. 2c. Larger shifts are seen in the film mode localized at the SiC/ SiO_2 interface, understandable as a result of increased in-plane confinement and a depression in frequency toward the pole in material $\chi^{(3)}$ at ω_{TO} . Utilising SiO_2 , a relatively low index substrate, leaves open the possibility of exciting this mode via prism coupling [21]. It was assumed that excitation occurred near critical coupling, so around 70% of the input beam coupled to the surface mode. A more complete approach, considering the surface modes self interaction as it propagates can be carried out by solving the Hopfield equations of motion including the nonlinearity, in the spirit of previous classical studies [26]. Now we refocus our discussion to the modes of nanometric resonators which have been predicted to support optical modes with ultra-small photonic mode volumes and correspondingly high energy localisation [14, 16]. Although here we study isolated resonators our results should

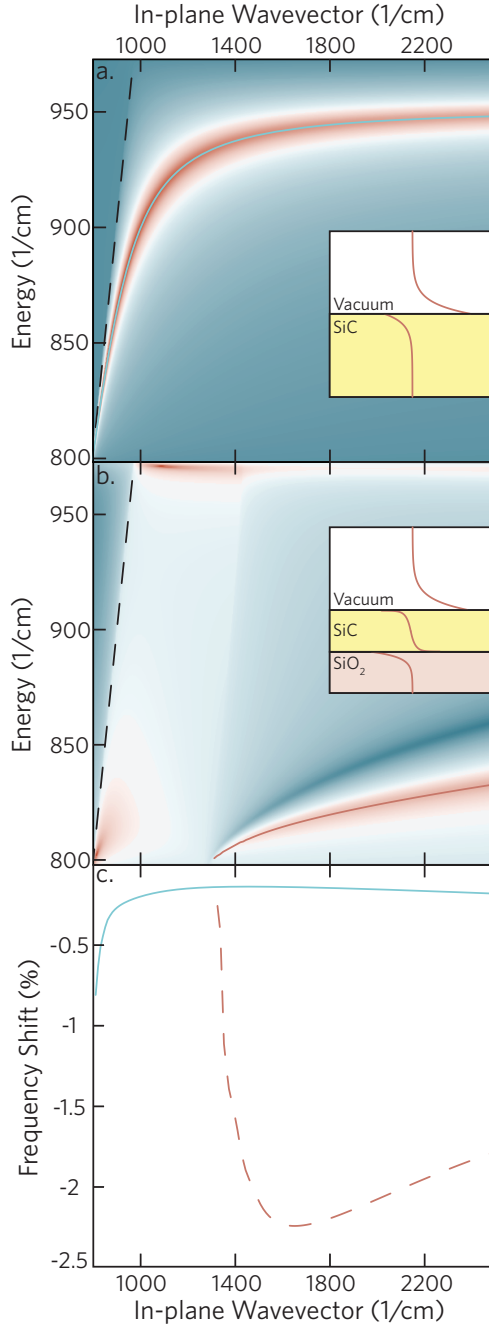


FIG. 2. a. Dispersion of the surface phonon polariton at the planar SiC/ vacuum interface illustrated in the inset. b. Dispersion of the surface phonon polariton on the SiO₂/ 100nm SiC/ vacuum trilayer shown in the inset. c. The self-phase-modulation frequency shift calculated for the bilayer mode (green solid line) and the low lying trilayer mode (red dashed line) from Eq. 4 for pump parameters representative of a free electron laser [21].

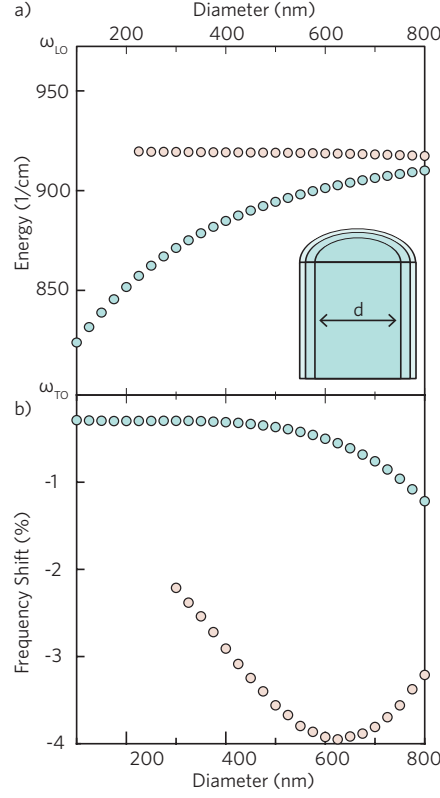


FIG. 3. a. Real resonant frequencies of the lowest order transverse ($m=1$, red circles) and longitudinal ($m=0$, blue circles) modes of a single, cylindrical resonator as a function of diameter. The cylinder height is held at 800nm. b. Fractional frequencies shifts for the same cylinder calculated by Eq. 4

provide an accurate approximation to those expected for experimentally practical resonator arrays [27]. The modes of such a resonator are easily probed utilising a numerical package such as COMSOL Multiphysics, allowing for evaluation of the integrated quantities entering Eq. 4. We focus here on the modes of sub-wavelength cylindrical resonators, which exhibit ultrasmall mode volumes less than $10^{-5}\lambda_0^3$ [14]. We study a cylinder as the diameter is varied from 800nm to 50nm. The modes of the cylinder vary azimuthally as $e^{im\phi}$. The modal frequencies for the lowest order longitudinal ($m = 0$) and transverse ($m = 1$) modes are shown in Fig. 3a. The transverse mode is weakly affected by the geometrical change as the cylinder is quasistatic for all sizes studied, while the longitudinal mode shifts to the transverse optic phonon frequency as the diameter tends to 0. In Fig. 3b we show the expected self-phase-modulation frequency shift. The expected shift for the transverse mode is far larger than for the longitudinal mode despite the longitudinal mode lying closer to the

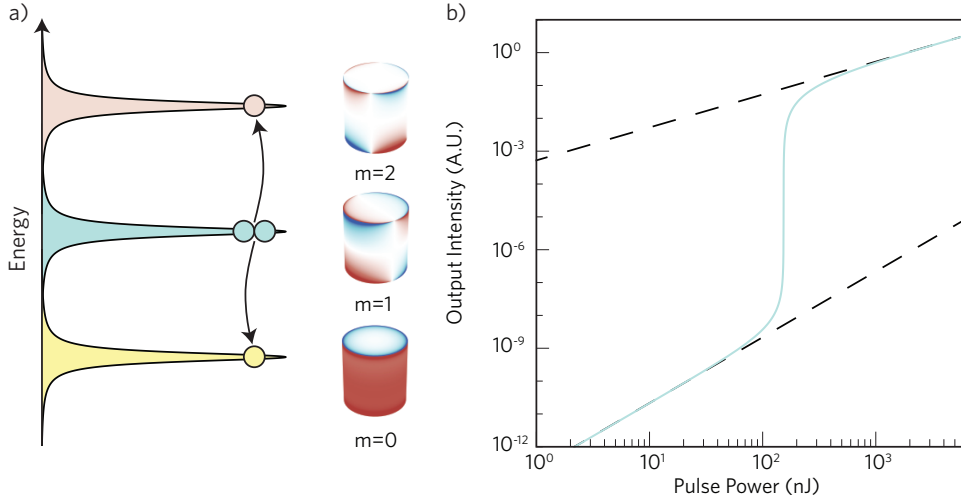


FIG. 4. a) An illustration of parametric scattering between 3 different modes. Two photons from the central branch with azimuthal dependance $e^{i\phi}$ scatter to one in the lower branch with azimuthal dependance $e^{0i\phi}$ and one in the upper branch with azimuthal dependance $e^{2i\phi}$. Illustrated on the right are the z -component of the electric field for these modes in a cylinder of height 800nm and of diameter 850nm. b) The solution of the rate equations in the steady state. Dashed lines indicate the quadratic and linear pumping of the output before and after threshold.

pole in the $\chi^{(3)}$ at ω_{TO} throughout. This is understandable as a result of increased optical confinement and modal overlap, expressed by the ratio $\mathcal{G}_p = V_{pp}^{\text{pp}}/V_p^2$.

B. Parametric Scattering

Having shown that the $\chi^{(3)}$ nonlinearity in SiC is expected to be large enough to lead to experimentally measurable effects, we pass to investigate the possibility to achieve a polariton parametric oscillator based on phonon-polaritons. Parametric oscillators exploit optical nonlinearities to convert photons from a pump beam oscillating into photons in signal and idler channels. This requires the three modes involved to respect phase matching conditions that can put strong constraints on the feasibility of practical devices. In microcavity polariton systems phase matching can be achieved at a magic angle, relying on the kink in the polariton dispersion [7], or utilising multiple cavities [8]. In this regards localised phonon polaritons are a much more flexible system in which to study parametric oscillation due to the morphologically dependant nature of their resonances.

Studying the general scattering process illustrated in Fig. 4, where two excitations in the central branch with frequency $\omega_{\mathbf{p}}$ scatter to one in the upper and one in the lower modes with frequencies $\omega_{\mathbf{p}_3}, \omega_{\mathbf{p}_4}$ respectively the scattering rate can be written utilising the Fermi golden rule. Here we calculate solely the spontaneous rate, assuming empty output channels

$$\mathcal{W} = \frac{6\pi\hbar^2\omega_{\mathbf{p}}^2\mathcal{N}_0^2}{\epsilon_0^2V_{\mathbf{p}}^2} \sum_{\mathbf{p}_i, \mathbf{p}_j} \sum_{\mathbf{p}_3, \mathbf{p}_4} \int d\omega_{\mathbf{p}_3} \omega_{\mathbf{p}_3} \rho_{\mathbf{p}_i}(\omega_{\mathbf{p}_3}) \times \int d\omega_{\mathbf{p}_4} \omega_{\mathbf{p}_4} \rho_{\mathbf{p}_j}(\omega_{\mathbf{p}_4}) \left| \chi_{ijkl}^{(3)}(\omega_{\mathbf{p}}, \omega_{\mathbf{p}}, \omega_{\mathbf{p}_3}, \omega_{\mathbf{p}_4}) \frac{\mathcal{V}_{\mathbf{pp}}^{\mathbf{p}_3 \mathbf{p}_4}}{\sqrt{V_{\mathbf{p}_3} V_{\mathbf{p}_4}}} \right|^2 \delta(2\omega_{\mathbf{p}} - \omega_{\mathbf{p}_3} - \omega_{\mathbf{p}_4}), \quad (6)$$

where \mathcal{N}_0 is the number of excitations in the pumped mode, $\mathcal{N}_L(\mathcal{N}_U)$ is that in the lower (upper) output channel and $\rho(\omega)$ represents the density of final states which is assumed to be Lorentzian

$$\rho_{\mathbf{p}_i}(\omega_{\mathbf{p}}) = \frac{1}{\pi} \frac{\text{Im}[\omega_{\mathbf{p}_i}]}{(\omega_{\mathbf{p}} - \text{Re}[\omega_{\mathbf{p}_i}])^2 + \text{Im}[\omega_{\mathbf{p}_i}]}, \quad (7)$$

for a mode with complex resonant frequency $\omega_{\mathbf{p}_i}$. The sum extends over all possible output modes $\mathbf{p}_i, \mathbf{p}_j$. Carrying out the integral over $\omega_{\mathbf{p}_4}$ yields

$$\mathcal{W} = \frac{6\pi\hbar^2\omega_{\mathbf{p}}^2\mathcal{N}_0^2}{\epsilon_0^2V_{\mathbf{p}}^2} \sum_{\mathbf{p}_i, \mathbf{p}_j} \int d\omega_{\mathbf{p}_3} \omega_{\mathbf{p}_3} \rho_{\mathbf{p}_i}(\omega_{\mathbf{p}_3}) \rho_{\mathbf{p}_j}(2\omega_{\mathbf{p}} - \omega_{\mathbf{p}_3}) (2\omega_{\mathbf{p}} - \omega_{\mathbf{p}_3}) \times \left| \chi_{ijkl}^{(3)}(\omega_{\mathbf{p}}, \omega_{\mathbf{p}}, \omega_{\mathbf{p}_3}, 2\omega_{\mathbf{p}} - \omega_{\mathbf{p}_3}) \frac{\mathcal{V}_{\mathbf{pp}}^{\mathbf{p}_3 \mathbf{p}_4}}{\sqrt{V_{\mathbf{p}_3} V_{\mathbf{p}_4}}} \right|^2, \quad (8)$$

which for well defined output states is only non-zero if the density of states are overlapped, implying that the system resonances are judiciously chosen to satisfy the parametric scattering condition $\text{Re}[\omega_{\mathbf{p}_i} + \omega_{\mathbf{p}_j}] = 2\omega_{\mathbf{p}}$.

Although our theory is applicable to any resonator geometry and can easily be applied to practical devices such as periodic arrays of resonators on a same material substrate where the analogy with microcavity polaritonics is most apparent [27] here we apply it to the illustrative system of an isolated cylindrical resonator. The energy requirement can be fulfilled when the diameter is 850nm. In this case we consider two transverse $m = 1$ modes scattering to one longitudinal $m = 0$ mode and one $m = 2$ mode as illustrated in Fig. 4. The real resonant frequencies are calculated utilising a pole-finding algorithm and the COMSOL multiphysics finite element solver to be 911.5/cm, 916.5/cm, 921.5/cm for the $m = 1, 2, 3$ modes respectively with Q-factors 123, 133, 154. The integral over the output modes can be carried out by the residue theorem, considering the poles of the two output density of

states in the upper halfspace, to find

$$\mathcal{W} = \frac{6\pi\hbar^2\omega_p^2\mathcal{N}_0^2}{\epsilon_0^2V_p^2} \times \left[\omega_{\mathbf{p}_i} (2\omega_{\mathbf{p}} - \omega_{\mathbf{p}_i}) \rho_{\mathbf{p}_j} (2\omega_{\mathbf{p}} - \omega_{\mathbf{p}_i}) \left| \chi_{ijkl}^{(3)} (\omega_{\mathbf{p}}, \omega_{\mathbf{p}}, \omega_{\mathbf{p}_i}, 2\omega_{\mathbf{p}} - \omega_{\mathbf{p}_i}) \frac{\mathcal{V}_{\mathbf{pp}}^{\mathbf{p}_i\mathbf{p}_4}}{\sqrt{V_{\mathbf{p}_i}V_{\mathbf{p}_4}}} \right|^2 \right. \right. \\ \left. \left. + \omega_{\mathbf{p}_j} (2\omega_{\mathbf{p}} - \omega_{\mathbf{p}_j}) \rho_{\mathbf{p}_i} (\omega_{\mathbf{p}_i}) \left| \chi_{ijkl}^{(3)} (\omega_{\mathbf{p}}, \omega_{\mathbf{p}}, \omega_{\mathbf{p}_j}, 2\omega_{\mathbf{p}} - \omega_{\mathbf{p}_j}) \frac{\mathcal{V}_{\mathbf{pp}}^{\mathbf{p}_j\mathbf{p}_4}}{\sqrt{V_{\mathbf{p}_j}V_{\mathbf{p}_4}}} \right|^2 \right] \right], \quad (9)$$

and assuming the $\chi^{(3)}$ to be roughly dispersionless over the modes, which is reasonable as they are detuned from it's pole at ω_{TO} we can write

$$\mathcal{W} = \frac{6\hbar^2\omega_p^2\mathcal{N}_0^2}{\epsilon_0^2V_p^2} \left| \chi_{ijkl}^{(3)} (\omega_{\mathbf{p}}, \omega_{\mathbf{p}}, \omega_{\mathbf{p}_j}, 2\omega_{\mathbf{p}} - \omega_{\mathbf{p}_j}) \frac{\mathcal{V}_{\mathbf{pp}}^{\mathbf{p}_j\mathbf{p}_4}}{\sqrt{V_{\mathbf{p}_j}V_{\mathbf{p}_4}}} \right|^2 [\omega_{\mathbf{p}_i}\mathcal{Q}_{\mathbf{p}_j} + \mathcal{Q}_{\mathbf{p}_i}\omega_{\mathbf{p}_j}], \quad (10)$$

where the \mathcal{Q} are the quality factors of the respective output modes. We can utilise this scattering rate, in conjunction with the known pump rate P_0 and loss rates calculated from simulations of the linear electromagnetics of the resonator to form a set of rate equations describing the population dynamics. On assuming the loss rates for each mode are approximately equal, so $\Gamma_0 \approx \Gamma_U \approx \Gamma_L = \Gamma$ we can write

$$\dot{\mathcal{N}}_0 = P_0 - \Gamma\mathcal{N}_0 - 2\mathcal{W}\mathcal{N}_0^2(\mathcal{N}_L + 1)^2 + 2\mathcal{W}\mathcal{N}_L^2(\mathcal{N}_0 + 1)^2, \quad (11)$$

$$\dot{\mathcal{N}}_L = -\Gamma\mathcal{N}_L - \mathcal{W}\mathcal{N}_L^2(\mathcal{N}_0 + 1)^2 + \mathcal{W}(\mathcal{N}_L + 1)^2\mathcal{N}_0^2, \quad (12)$$

where we simplified by noticing that equal damping rates implies $\mathcal{N}_L = \mathcal{N}_U$. We can find the threshold condition for amplification by rewriting the evolution equation for the lower channel as

$$\dot{\mathcal{N}}_L = \mathcal{N}_L (\mathcal{R}_{\text{in}} - \mathcal{R}_{\text{out}}) + \mathcal{R}_{\text{in}}, \quad (13)$$

and as at threshold we expect $\mathcal{R}_{\text{in}} = \mathcal{R}_{\text{out}}$ we can write

$$\mathcal{N}_L = \frac{\mathcal{W}\mathcal{N}_0 - \Gamma}{\mathcal{W}(2\mathcal{N}_0 + 1)}, \quad (14)$$

finding the threshold condition $\mathcal{N}_0 = \sqrt{\frac{\Gamma}{\mathcal{W}}}$ and corresponding threshold pump rate

$$P_{\text{th}} = \Gamma \sqrt{\frac{\Gamma}{\mathcal{W}}} \approx 5.8 \times 10^{19} \text{ s}^{-1} \quad (15)$$

from which we can calculate the required energy per pulse utilising the free-electron lasers characteristic pulse length and spot size extrapolated to continuous wave pumping as 218nJ.

We can also solve the coupled rate equations in the steady state, the solution for \mathcal{N}_L is shown in Fig. 4b, showing the onset of parametric scattering around the calculated threshold pulse power P_{th} and a corresponding transition from quadratic to linear pumping of the output. As the power emitted in a single pulse can reach $1\mu\text{J}$ [21] this hints tantalisingly that such processes are experimentally attainable in such sub-diffraction resonator systems. While the need to conserve azimuthal mode number m through the scattering process makes the system chosen in this Letter seem rather restrictive, this is only one particular set of modes, chosen for sake of simplicity. Conservation of energy and in-plane momentum could in fact be achieved by coupling the modes of discrete surface phonon resonators to propagative surface phonon polaritons on a planar interface [27]. In this system it would be possible to utilise a single resonator mode for the input and the outputs, analogous to a microcavity polariton system, possibly increasing the overlap \mathcal{V} in the process.

IV. CONCLUSION

In conclusion, we have presented a theory of four-wave-mixing in arbitrary phonon-polariton resonators. We applied this theory to the measurement of self-phase-modulation [26] for both propagative and localised modes, showing that the relevant shifts are within experimental reach. We further studied parametric scattering between discrete resonator modes, again showing parametric oscillator regime is achievable for reasonable experimental parameters. The theory considered above can be easily applied to realistic experimental geometries [16] where phase matching can be achieved by hybridising the modes of discrete resonators with a propagating phonon polariton.

[1] Houdré, R.; Stanley, R. P.; Oesterle, U.; Illegems, M.; Weisbuch, C. Room-temperature cavity polaritons in a semiconductor microcavity. *Phys. Rev. B* 1994, **49**, 16761.

[2] Lidzey, D. G.; Bradley, D. D. C.; Skolnick, M. S.; Virgili, T.; Walker, S.; Whittaker, D. M. Strong exciton-photon coupling in an organic semiconductor microcavity. *Nature* 1998, **395**, 53-55.

[3] Kasprzak, J.; Richard, M.; Kundermann, S.; Baas, A.; Jeambrun, P.; Keeling, J. J. M.; Marchett, F. M.; Szymańska, M. H.; André, R.; Staehli, J. L.; Savona, V.; Littlewood, P. B.;

Deveaud, B.; Dang, L. S. Bose-Einstein condensation of exciton polaritons. *Nature* 2006, **443**, 409-414.

[4] Daskalakis, K. S.; Maier, S. A.; Murray, R.; Kéna-Cohen, S. Nonlinear interactions in an organic polariton condensation. *Nat. Mat.* 2014, **13**, 271-278.

[5] Amo, A.; Sanvitto, D.; Laussy, F. P.; Ballarini, D.; del Valle, E.; Martin, M. D.; Lemaître, A.; Bloch, J.; Krizhanovskii, D. N.; Skolnick, M. S.; Tejedor, C.; Viña, L. Collective fluid dynamics of a polariton condensate in a semiconductor microcavity. *Nature* 2009, **457**, 291-295.

[6] Lerario, G.; Fieramosa, A.; Barachati, F.; Ballarini, D.; Daskalakis, K. S.; Dominici, L.; De Giorgi, M.; Maier, S. A.; Gigli, G.; Kéna-Cohen, S.; Sanvitto, D. Room-temperature superfluidity in a polariton condensate. *arXiv* 2016, 1609.03153.

[7] Baumberg, J. J.; Savvidis, P. G.; Stevenson, R. M.; Tartakovskii, A. I.; Skolnick, M. S.; Whittaker, D. M.; Roberts, J. S. Parametric oscillation in a vertical microcavity: A polariton condensate or micro-optical parametric oscillation. *Phys. Rev. B* 2000, **62**, R16247.

[8] Diederichs, C.; Tignon, J.; Dasbach, G.; Ciuti, C.; Lemaître, A.; Bloch, J.; Roussignol, P.; Delalande, C. Parametric oscillation in vertical triple microcavities. *Nature* 2006, **440**, 904-907.

[9] Schneider, C.; Rahimi-Iman, A.; Kim, N. Y.; Fischer, J.; Savenko, I. G.; Amthor, M.; Lermer, M.; Wolf, A.; Worschech, L.; Kulakovskii, V. D.; Shelykh, I. A.; Kamp, M.; Reitzenstein, S.; Forchel, A.; Yamamoto, Y.; Höfling, S. An electrically pumped polariton laser. *Nature* 2013, **497**, 348-352.

[10] Bhattacharya, P.; Xiao, B.; Das, A.; Bhowmick, S.; Heo, J. Solid state electrically injected exciton-polariton laser. *Phys. Rev. Lett.* 2013, **110**, 206403.

[11] Khurgin, J. How to deal with the loss in plasmonics and metamaterials. *Nature Nanotechnology* 2015, **10**, 2-6.

[12] Caldwell, J. D.; Lindsay, L.; Giannini, V.; Vurgaftman, I.; Reinecke, T. L.; Maier, S. A.; Glembotck, O. J. Low-loss, infrared and terahertz nanophotonics using surface phonon polaritons. *Nanophotonics* 2015, **4**, 44-68.

[13] Schuller, J. A.; Taubner, T.; Brongersma, M. L.; Optical antenna thermal emitters. *Nature Photonics* 2009, **3**, 658-661.

[14] Gubbin, C. R.; Maier, S. A.; De Liberato, S. Theoretical Investigation of Phonon Polaritons in SiC Micropillar Resonators. *Phys. Rev. B* 2017, **95**, 035313.

[15] Caldwell, J. D.; Glebocki, O. J.; Francescato, Y.; Sharac, N.; Giannini, V.; Bezares, F. J.; Long, J. P.; Owrusky, J. C.; Vurgaftman, I.; Tischler, J. G.; Wheeler, V. G.; Bassim, N. B.; Shirey, L. M.; Kasica, R.; Maier, S. A. Low-Loss, Extreme Subdiffraction Photon Confinement via Silicon Carbide Localized Surface Phonon Polariton Microresonators. *Nano Lett.* 2013, **13**, 3690-3697.

[16] Chen, Y.; Francescato, Y.; Caldwell, J. D.; Giannini, V.; Maß, T. W. W.; Glebocki, O. J.; Bezares, F. J. Taubner, T.; Kasica, R.; Hong, M.; Maier, S. A. Spectral Tuning of Localized Surface Phonon Polariton Resonators for Low-loss Mid-IR Applications. *ACS Phot.* 2014, **1**, 718-724.

[17] Hopfield, J. J. Theory of the Contribution of Excitons to the Complex Dielectric Constant of Crystals. *Phys. Rev.* 1958, **112**, 1555-1567.

[18] Gubbin, C. R.; Maier, S. A.; De Liberato, S. Real-Space Hopfield Diagonalization of Inhomogeneous Dispersive Media. *Phys. Rev. B* 2016, **94**, 205301.

[19] Gubbin, C. R.; De Liberato, S.; Theory of nonlinear polaritonics: $\chi^{(2)}$ scattering on a β -SiC surface. *ACS Photonics* 2017, **4**, 1381-1388.

[20] Paarmann, A.; Razdolski, I.; Gewinner, S.; Schöllkopf, W.; Wolf, M. Effects of Crystal Anisotropy on Optical Phonon Resonances in Midinfrared Second Harmonic Response of SiC. *Phys. Rev. B* 2016, **94**, 134312.

[21] Passler, N. C.; Razdolski, I.; Gewinner, S.; Schöllkopf, W.; Wolf, M.; Paarmann, A. Second-Harmonic Generation from Critically Coupled Surface Phonon Polaritons. *ACS Photonics* 2017, **4**, 1048-1053.

[22] Razdolski, I.; Chen, Y.; Giles, A. J.; Gewinner, S.; Schöllkopf, W.; Hong, M.; Wolf, M.; Giannini, V.; Caldwell, J. D.; Maier, S. A.; Paarmann, A.; Resonant Enhancement of Second-Harmonic Generation in the Mid-Infrared Using Localized Surface Phonon Polaritons in Sub-diffractive Nanostructures. *Nano Lett.* 2016, **16**, 6954-6959.

[23] De Leon, I.; Sipe, J. E.; Boyd, R. W. Self-phase-modulation of surface plasmon polaritons. *Phys. Rev. A* 2014, **89**, 013855.

[24] Vanderbilt, D.; Louie, S. G.; Cohen, M. L. Calculation of Anharmonic Phonon Couplings in C, Si and Ge. *Phys. Rev. B* 1986, **33**, 8740-8747.

[25] Taubner, T.; Korobkin, D.; Urzhumov, Y.; Shvets, G.; Hillenbrand, R. Near-field Microscopy Through a SiC Superlens. *Science* 2006, **313**, 1595.

- [26] De Leon, I.; Shi, Z.; Liapis, A. C.; Boyd, R. W. Measurement of the complex nonlinear optical response of a surface plasmon-polariton. *Opt. Lett.* 2014, **39**, 2274-2277.
- [27] Gubbin, C. R.; Martini, F.; Politi, A.; Maier, S. A.; De Liberato, S. Strong and Coherent Coupling Between Localised and Propagating Phonon Polaritons. *Phys. Rev. Lett.* 2016, **116**, 246402.